Magnetic anisotropy in single-crystal rare-earth-doped $R Ba_2Cu_4O_8$ (R = Y, Dy, Gd, Ho, Er, Tm, Yb)

D. H. Nichols
National High Magnetic Field Laboratory, Florida State University, Tallahassee, Florida 32306

B. Dabrowski
Department of Physics, Northern Illinois University, Dekalb, Illinois 60115

U. Welp
Material Science Division, Argonne National Laboratory, Argonne, Illinois 60439

J. E. Crow
National High Magnetic Field Laboratory, Florida State University, Tallahassee, Florida 32306
(Received 29 September 1993)

We measured magnetic susceptibility of single-crystal rare-earth-doped $R Ba_2Cu_4O_8$ (where R = Y, Dy, Gd, Ho, Er, Tm, Yb) in the normal state along the three principal axes. The anisotropy measured fits well to calculated values obtained from crystal electric field (CEF) analysis. From our results we developed a general scaling relation for the CEF parameters across the rare-earth series.

INTRODUCTION

One of the unique properties of the high-T_c oxide superconductors, $R Ba_2Cu_3O_7$, is that substitution of most of the rare-earth elements for Y does not significantly change the superconducting transition temperature T_c. This is true even though most of the R ions have partially filled f-electron shells and associated magnetic moments. In the conventional theory of superconductors containing magnetic impurities[1] a small amount of impurities causes a drastic suppression of T_c. Therefore it has been argued[2] that the R ion is well localized between the CuO_2 planes and isolated from the superconducting electrons residing in the CuO_2 planes. An understanding of the magnetic ordering of the rare-earth-ion sublattice which coexists with the superconductivity requires a knowledge of the crystal-electric-field (CEF) states of the R ion. Along with a measure of the anisotropy we performed a crystalline-electric-field analysis to determine the energy splitting of the rare-earth ion in the 1:2:4 structure and the best-fit crystal-field parameters. From our results we developed a scaling relation for the crystal-field parameters across the rare-earth series.

To investigate further this apparent decoupling of the R ions and the superconducting electrons without the added complication of the uncertainty of oxygen stoichiometry that often plagues the 1:2:3 system we turned to the 1:2:4 system. The site symmetry of the rare-earth ion in the 1:2:3 and 1:2:4 systems is very similar, making an analysis of the one in terms of the other reasonable. The 1:2:4 structure has an additional Cu-O chain layer in the unit cell and a doubling of the unit cell in the c direction.[3] The oxygen stoichiometry of the 1:2:4 system is much more stable than that of the 1:2:3.

The variable oxygen stoichiometry of the 1:2:3 phase adds an additional unknown variable making interpretation of the physical data difficult. For this reason the 1:2:4 phase lends itself better to analysis. Magnetic measurements were made in the normal state from $100 < T < 350$ K on single-crystal $R Ba_2Cu_4O_8$ samples along the three principal axes of the crystal, with R = Y, Gd, Er, Dy, Ho, Tm, Yb.

EXPERIMENT

Single crystals of $R Ba_2Cu_4O_8$ were grown by a flux method described by Dabrowski *et al.*[4] The samples were first characterized by examining the crystals under a polarized light microscope. This technique relies on the small difference in the phase of the reflected light when it is polarized along the a and b axes.[5] We used this technique to screen out crystals which had inclusions or c-axis twins in which the a and b axes interchange while moving up the c axis. This technique was checked against an x-ray analysis on one of the crystals to confirm our determination of the a and b axes of the crystals. Second, we measured the magnetization in a low-field superconducting quantum interference device (SQUID) magnetometer in a field of 1 Oe from $4 < T < 100$ K. We determined the quality of the samples based on T_c, width of the transition, and bulk magnetization. We performed normal-state magnetization measurements in a (Quantum Design) SQUID magnetometer in a field of 10 kOe from $100 < T < 350$ K. By mounting the crystal on a quartz fiber oriented parallel to the field, we performed magnetization measurements along the three principal axes of the crystal. This mounting technique has the advantage of a negligible background signal and no variation of the sample centering due to thermal expansion.[6]

0163-1829/94/49(13)/9150(7)/$06.00

©1994 The American Physical Society

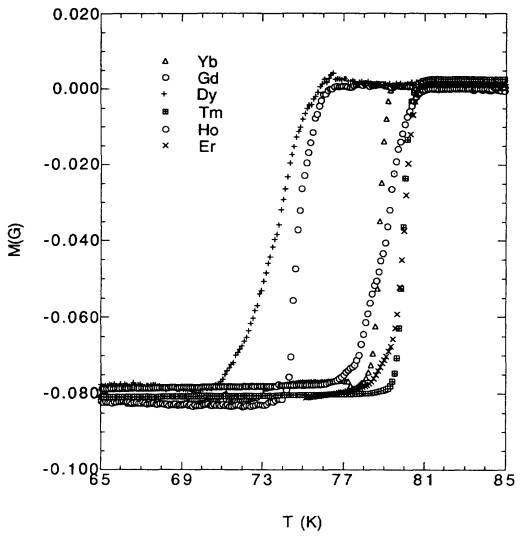

FIG. 1. Magnetization vs temperature in a field of 1 Oe.

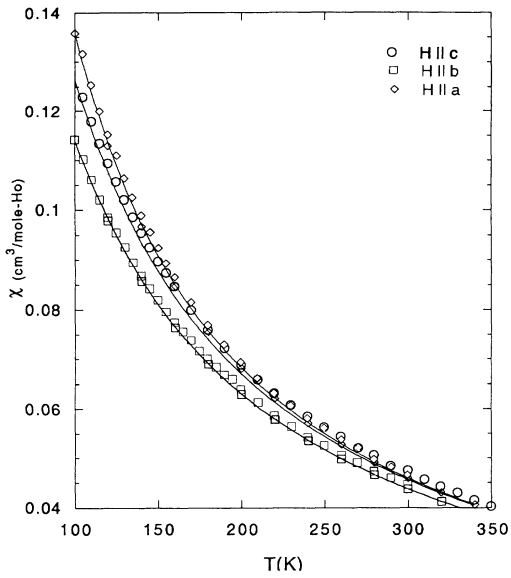

FIG. 2. $\chi(T)$ vs T for $HoBa_2Cu_4O_8$ along the three principal axes. The solid lines are the theoretical fits.

RESULTS

Plotted in Fig. 1 is the dc magnetization of the $RBa_2Cu_4O_8$ single crystals measured below T_c in a field of 1 Oe where we first zero-field cooled to 4 K before the measurement. T_c values are consistent with the values measured by Morris *et al.*[7] Table I lists the values of T_c for our samples. In the case of Gd 1:2:4 the theoretical and measured anisotropy was very small, as is to be expected for an ion with an angular momentum quantum number $L=0$. An ion in this state should not experience any quenching of the magnetic moment. However, the measured moment was found to be 10% smaller than the free-ion value. An energy-dispersive-spectroscopy measurement on the crystal showed that it contained approximately 10% yttrium. This contamination resulted from growing the crystals in yttrium-stabilized zirconium crucibles at high temperatures. Therefore the data taken for all the samples was weighted to take into account this contamination.

The measured moment has contributions from core diamagnetism, itinerant magnetism, and the orbital and spin components from the various ions in the lattice. In order to isolate the R moment contribution we subtracted the measured moment of the nonmagnetic analog $YBa_2Cu_4O_8$ (Ref. 6) from the R 1:2:4 data. For $YBa_2Cu_4O_8$ at 150 K, $\chi_a=2.5\times10^{-4}$, $\chi_b=1.7\times10^{-4}$, $\chi_c=3.6\times10^{-4}$ cm^3/mole Y), showing that all contributions besides the R moment are negligible. Plotted in Figs. 2–7 are the net susceptibilities and the theoretical fits for the three field directions based on a CEF analysis.

TABLE I. Table of measured T_c's for R 1:2:4.

Compound	T_c (K)
$YBa_2Cu_4O_8$	80.0
$GdBa_2Cu_4O_8$	74.7
$DyBa_2Cu_4O_8$	73.6
$HoBa_2Cu_4O_8$	79.0
$ErBa_2Cu_4O_8$	80.0
$TmBa_2Cu_4O_8$	79.9
$YbBa_2Cu_4O_8$	78.8

The CEF analysis was based on the Hamiltonian

$$H_{\mathrm{CEF}}=\sum B_m^n O_m^n \ .$$

The B_m^n's are called the crystalline-electric-field parameters and are related to the radial moments of the magnetic ion $B_m^n=A_m^n\langle r^n\rangle$. These parameters are difficult to calculate and so are determined by experiment. The O_m^n's are angular momentum operators and are functions of

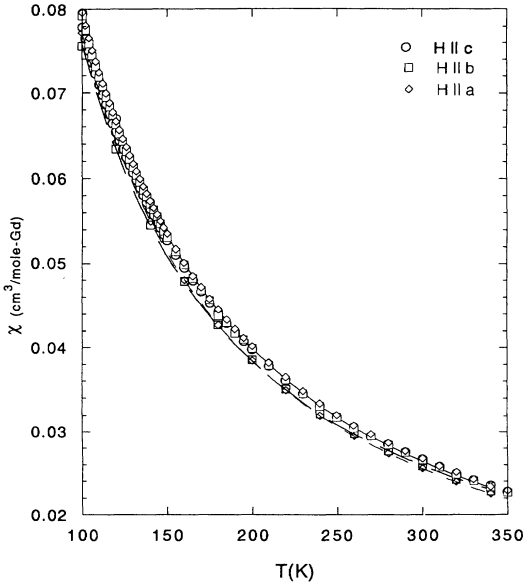

FIG. 3. $\chi(T)$ vs T for $GdBa_2Cu_4O_8$ along the three principal axes. The solid lines are the theoretical fits.

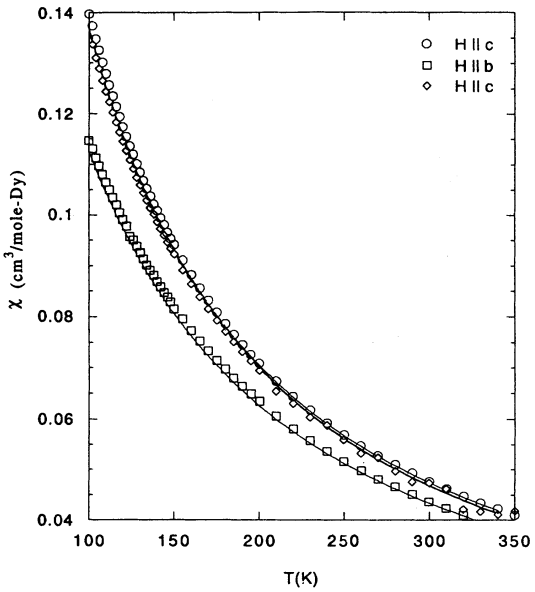

FIG. 4. $\chi(T)$ vs T for $DyBa_2Cu_4O_8$ along the three principal axes. The solid lines are the theoretical fits.

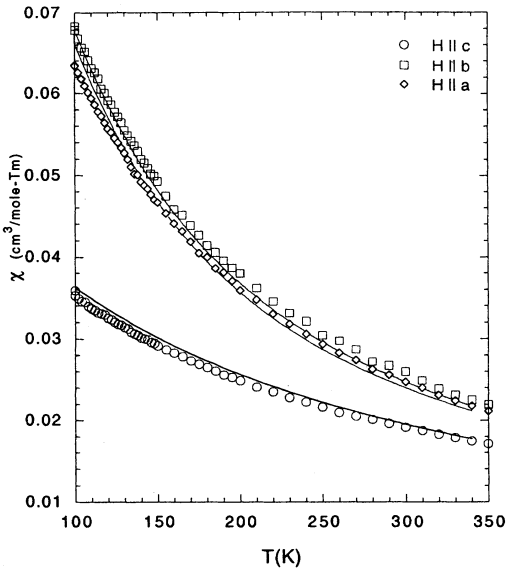

FIG. 6. $\chi(T)$ vs T for $TmBa_2Cu_4O_8$ along the three principal axes. The solid lines are the theoretical fits.

$O_m^n(J,J_z,J^+,J^-)$. This form of the Hamiltonian is based on the Stevens operator method.[8] The CEF analysis was based on a computer program using the Stevens operator method to generate the CEF Hamiltonian.[9] We obtained the starting crystal-field parameters from inelastic-neturon-scattering experiments performed on Er 1:2:3 and Ho 1:2:3.[10,11]

We diagonalized the Hamiltonian within the basis of the ground-state J multiplet of each of the rare earths under consideration. Therefore the eigenstates are written as a superposition of the base states $|\Gamma_i\rangle = \sum_{M=-J_z}^{J_z} a_M^i |M\rangle$. This is a good approximation because in the case of the heavy rare earths the energy splitting of the ground state is much smaller than the energy separation to the first excited multiplet.[12] The magnetic susceptibility is calculated using the Van Vleck formalism.[13]

$$\chi = \frac{N\mu\beta^2}{3\kappa_B TZ} \sum_{n,i} \left[\sum_j |\langle \Gamma_{n,i}|\mu|\Gamma_{n,j}\rangle|^2 - 2 \sum_{j,m\neq n} \frac{|\langle \Gamma_{n,i}|\mu|\Gamma_{m,j}\rangle|^2 \kappa_B T}{E_n - E_m} \right] \times \exp(-E_n/\kappa_B T) ,$$

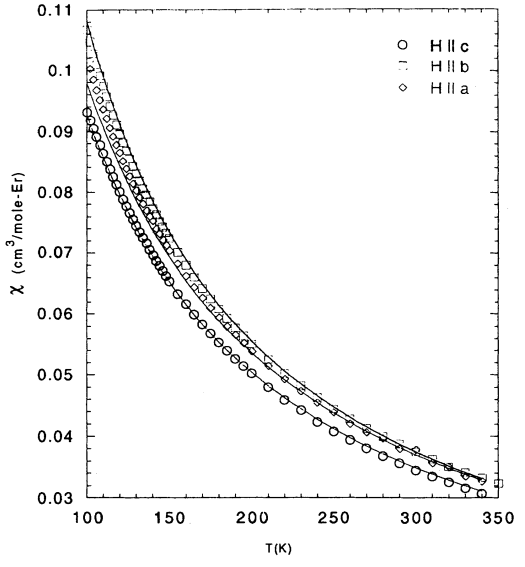

FIG. 5. $\chi(T)$ vs T for $ErBa_2Cu_4O_8$ along the three principal axes. The solid lines are the theoretical fits.

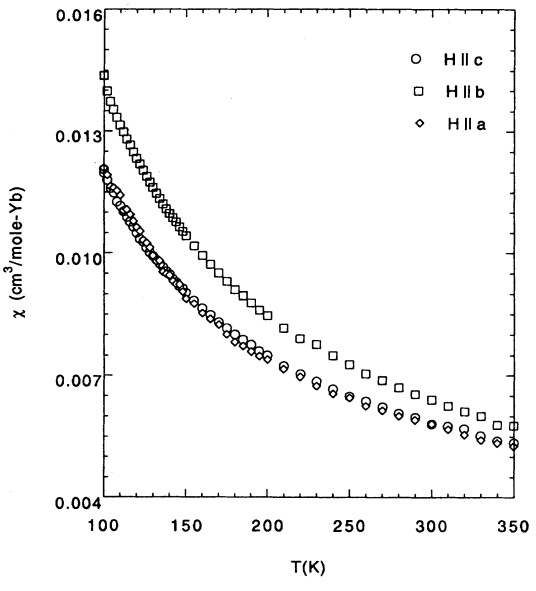

FIG. 7. $\chi(T)$ vs T for $YbBa_2Cu_4O_8$ along the three principal axes. The solid lines are the theoretical fits.

TABLE II. Initial starting parameters and best-fit final CEF parameters for R 1:2:4 in meV.

Compound		Gd 124	Dy 124	Ho 124[a]	Er 124[b]	Tm 124
B_{20}	Initial	-1.1×10^{-3}	-1.4×10^{-1}	-4.6×10^{-2}	5.1×10^{-2}	4.1×10^{-2}
	Final	-1.9×10^{-2}	-3.0×10^{-2}	-1.0×10^{-3}	3.0×10^{-2}	8.0×10^{-2}
B_{22}	Initial	-1.2×10^{-2}	-6.0×10^{-2}	-2.0×10^{-2}	5.8×10^{-2}	4.5×10^{-2}
	Final	-3.5×10^{-2}	-3.3×10^{-2}	-1.1×10^{-2}	3.0×10^{-3}	4.0×10^{-2}
B_{40}	Initial	1.2×10^{-3}	1.8×10^{-3}	9.1×10^{-1}	-1.3×10^{-3}	-3.7×10^{-3}
	Final	1.2×10^{-3}	1.8×10^{-3}	9.1×10^{-4}	-1.3×10^{-3}	-3.7×10^{-3}
B_{42}	Initial	-7.8×10^{-5}	-1.2×10^{-4}	-6.0×10^{-5}	-1.7×10^{-5}	2.5×10^{-4}
	Final	-7.8×10^{-5}	-1.2×10^{-4}	-6.0×10^{-5}	-1.7×10^{-4}	2.5×10^{-4}
B_{44}	Initial	-5.5×10^{-3}	-8.1×10^{-3}	-4.2×10^{-3}	7.7×10^{-3}	1.7×10^{-2}
	Final	-5.5×10^{-3}	-8.1×10^{-3}	-4.2×10^{-3}	7.6×10^{-3}	1.7×10^{-2}
B_{60}	Initial	-8.8×10^{-6}	4.1×10^{-6}	-4.5×10^{-6}	7.4×10^{-6}	-1.5×10^{-5}
	Final	-8.8×10^{-6}	4.1×10^{-6}	-4.5×10^{-3}	7.4×10^{-6}	-1.5×10^{-5}
B_{62}	Initial	5.3×10^{-6}	-2.5×10^{-6}	2.7×10^{-6}	9.3×10^{-6}	8.9×10^{-6}
	Final	5.3×10^{-6}	-2.5×10^{-6}	2.7×10^{-6}	9.3×10^{-6}	8.9×10^{-6}
B_{64}	Initial	-2.6×10^{-4}	1.2×10^{-4}	-1.4×10^{-4}	9.2×10^{-6}	-4.5×10^{-4}
	Final	-2.6×10^{-4}	1.2×10^{-4}	-1.4×10^{-4}	2.1×10^{-4}	-4.5×10^{-4}
B_{66}	Initial	3.7×10^{-6}	-1.7×10^{-6}	1.9×10^{-6}	2.2×10^{-4}	6.3×10^{-6}
	Final	3.7×10^{-6}	-1.7×10^{-6}	1.1×10^{-6}	4.0×10^{-6}	6.3×10^{-6}

[a]Reference 11.
[b]Reference 10.

where $Z=\sum_n d_n \exp(-E_n/\kappa_B T)$. Here $\Gamma_{n,l}$ are the d_n degenerate eigenfunctions of the CEF Hamiltonian with energy E_n in the absence of a magnetic field and $\mu=L+S$ is the magnetic-moment operator. We allowed the second-order crystal-filed parameters to vary using a Newton-Raphson root-finding technique[14] in order to minimize the χ^2 value. In the case of Er and Ho, some adjustment by hand in the sixth-order parameters was necessary in order to optimize the fit. We obtained starting parameters for each rare earth by scaling the radial moments and Stevens multiplicative factors from Ho 1:2:3 and Er 1:2:3. For instance, to obtain starting CEF parameters for Tm 1:2:4,

$$B_m^n(\mathrm{Tm})=B_m^n(\mathrm{Er})\frac{\langle r^n\rangle_{\mathrm{Tm}}}{\langle r^n\rangle_{\mathrm{Er}}}\frac{\theta_n(\mathrm{Er})}{\theta_n(\mathrm{Tm})}$$

where $\langle r^n\rangle$ are the radial moments in units of a_0^{-n} and θ_n are the Stevens multiplicative factors of each rare earth. The values of $\langle r^n\rangle$ and θ_n can be found in.[15] These procedures were performed on $R\mathrm{Ba_2Cu_4O_8}$ with $R=$ Gd, Dy, Ho, Er, Tm, Yb.

TABLE III. Calculated energy levels of Ho^{3+} in $HoBa_2Cu_4O_8$ from the CEF parameters for each eigenstate Γ_m^n.

Symmetry	E_{calc} (meV)	E_{meas} (meV)[a]
Γ_1^5	71.5	73.1
Γ_4^4	70.4	. . .
Γ_2^4	70.2	70.0
Γ_1^4	63.9	. . .
Γ_2^3	63.3	59.0
Γ_4^3	58.1	59.0
Γ_3^4	57.9	. . .
Γ_1^3	57.0	. . .
Γ_3^3	56.4	. . .
Γ_4^2	11.4	11.6
Γ_2^2	10.8	10.8
Γ_1^2	8.8	8.1
Γ_3^2	5.0	4.3
Γ_1^1	4.6	3.8
Γ_2^1	1.9	1.8
Γ_4^1	0.9	0.5
Γ_3^1	0.0	. . .

[a]Reference 11.

TABLE IV. Calculated energy levels of Gd^{3+} in $GdBa_2Cu_4O_8$ from the CEF parameters for each eigenstate Γ_m^n.

Symmetry	E_{calc} (meV)
Γ_8^6	2.5
Γ_8^5	2.5
Γ_8^4	1.3
Γ_8^3	1.3
Γ_5^2	0.8
Γ_5^1	0.8
Γ_8^2	0.0
Γ_8^1	0.0

TABLE V. Calculated energy levels of Dy^{3+} in $DyBa_2Cu_4O_8$ from the CEF parameters for each eigenstate Γ_m^n.

Symmetry	E_{calc} (meV)	E_{meas} (meV)[a]
Γ_5^8	67.5	. . .
Γ_5^7	65.0	. . .
Γ_5^6	53.8	. . .
Γ_5^5	16.2	17.0
Γ_5^4	12.6	14.0
Γ_5^3	2.4	5.9
Γ_5^2	1.2	3.3
Γ_5^1	0.0	0.0

[a]Reference 18.

TABLE VI. Calculated energy levels of Er^{3+} in $ErBa_2Cu_4O_8$ from the CEF parameters for each eigenstate Γ_m^n.

Symmetry	E_{calc} (meV)	E_{meas} (meV)[a]
Γ_5^8	77.5	81.0
Γ_5^7	74.3	77.0
Γ_5^6	70.8	72.5
Γ_5^5	66.3	67.5
Γ_5^4	11.3	11.0
Γ_5^3	9.7	9.8
Γ_5^2	9.6	9.4
Γ_5^1	0.0	0.0

[a]Reference 10.

TABLE VII. Calculated energy levels of Tm^{3+} in $TmBa_2Cu_4O_8$ from the CEF parameters for each eigenstate Γ_m^n.

Symmetry	E_{calc} (meV)
Γ_4^3	67.2
Γ_2^3	66.7
Γ_1^3	66.7
Γ_1^3	65.1
Γ_3^3	62.5
Γ_2^2	61.3
Γ_4^2	59.0
Γ_3^2	28.9
Γ_1^2	20.1
Γ_1^1	19.0
Γ_2^1	11.8
Γ_4^1	11.8
Γ_3^1	0

TABLE VIII. CEF parameters in meV as a function of radial moment in units of a_0^{-n}.

$$B_{20}=8.7\times10^{-1}-1.3r^2$$
$$B_{22}=5.5\times10^{-1}-8.0\times10^{-1}r^2$$
$$B_{40}=-2.3\times10^{-2}+1.9\times10^{-2}r^4$$
$$B_{42}=1.2\times10^{-3}-1.0\times10^{-3}r^4$$
$$B_{44}=1.1\times10^{-1}-9.0\times10^{-2}r^4$$
$$B_{60}=-4.4\times10^{-5}+9.4\times10^{-6}r^6$$
$$B_{62}=3.6\times10^{-5}-7.5\times10^{-6}r^6$$
$$B_{64}=-1.1\times10^{-3}+2.5\times10^{-4}r^6$$
$$B_{66}=2.3\times10^{-5}-4.8\times10^{-6}r^6$$

TABLE IX. CEF parameters in meV as a function of cell volume (V) in units of $Å^3$.

$$B_{20}=11.7-2.9\times10^{-2}V$$
$$B_{22}=7.7-1.9\times10^{-2}V$$
$$B_{40}=-6.0\times10^{-1}+1.5\times10^{-3}V$$
$$B_{42}=4.0\times10^{-2}-9.9\times10^{-5}V$$
$$B_{44}=2.8-6.8\times10^{-3}V$$
$$B_{60}=-1.9\times10^{-3}+4.7\times10^{-6}V$$
$$B_{62}=1.1\times10^{-3}-2.8\times10^{-6}V$$
$$B_{64}=-5.8\times10^{-2}+1.4\times10^{-4}V$$
$$B_{66}=8.1\times10^{-4}-2.0\times10^{-6}V$$

Listed in Table II are the initial starting parameters and the best-fit CEF parameters from a CEF analysis performed on the data. Tables III–VII contain the energy eigenvalues and the symmetry classification of each state $\Gamma_{n,l}$. The close agreement between the energy eigenvalues obtained in this work and those obtained from inelastic neutron scattering is quite remarkable. A comparison of our Dy 1:2:4 CEF parameters to Dy 1:2:4 parameters obtained by neutron scattering[16] shows an agreement in the sign except in the case of the B_{66} parameter, which however does not weigh heavily in the outcome of the susceptibility calculation. The magnitudes of these Dy 1:2:4 CEF parameters however vary by as much as a factor of 40. This variation in magnitude should not be so surprising, however, because of the large number of fitting parameters, making the final fit parameters not unique. Using the parameters from Ref. 16 in a susceptibility calculation resulted in a poor fit to the experimental magnetic-susceptibility data, unlike the parameters obtained in this work which resulted in a very good fit. An unsuccessful attempt was made to fit the data for the Yb 1:2:4 sample in a CEF analysis. The calculation was per-

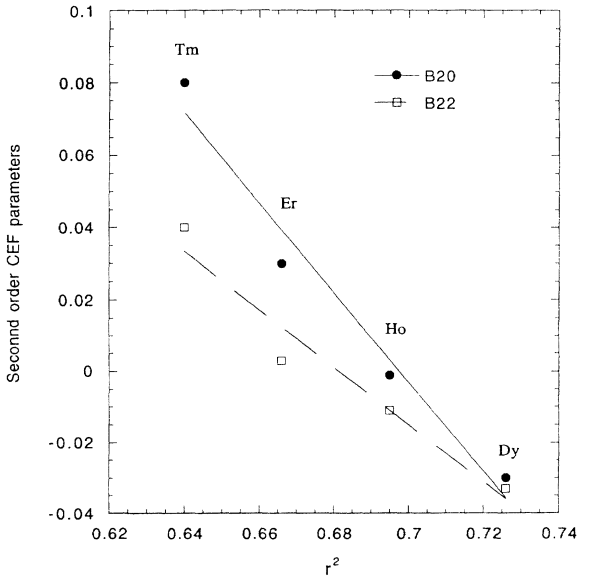

FIG. 8. Graph of second-order best-fit CEF parameters in meV vs second-order radial moment in units of a_0^{-2}.

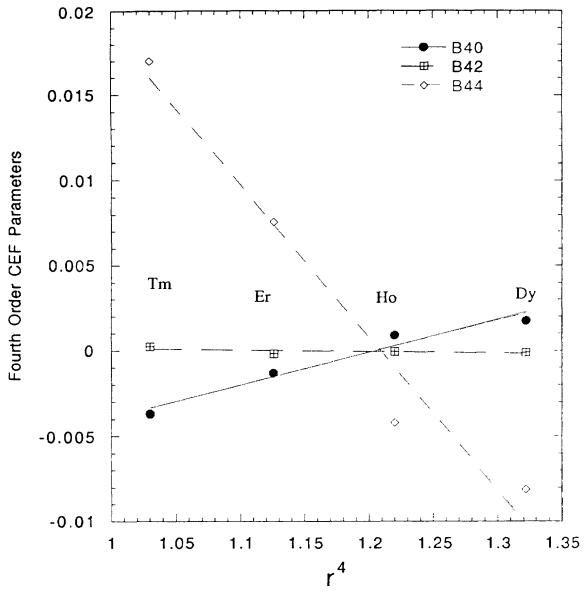

FIG. 9. Graph of fourth-order best-fit CEF parameters in meV vs fourth-order radial moment in units of a_0^{-2}.

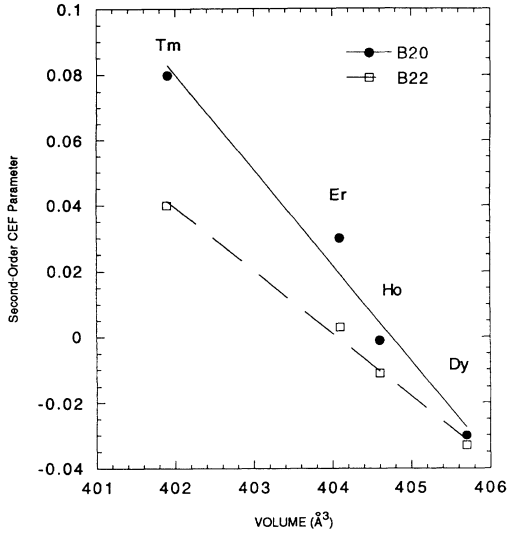

FIG. 11. Graph of second-order best-fit CEF parameters in meV vs cell volume in units of Å^3.

formed in another way by assuming a valence of 2+ for Yb. In this case the fit was even worse. The reason for the poor fit is not clear at this time. A comparison of the measured magnetic anisotropy in the 1:2:4 system with that in the 1:2:3 system would be desirable, but to our knowledge no such data exists. The measured easy axis agrees with that measured in aligned powder of $R\text{Ba}_2\text{Cu}_3\text{O}_7$.[17] As in the case of the aligned powders, the easy axis of the R 1:2:4 crystals correlates with the sign of the second-order Stevens factor θ_2.

We developed a generalized scaling relation for the CEF parameters between the $R\text{Ba}_2\text{Cu}_4\text{O}_8$ compounds in two ways. First, by plotting the best-fit crystal-field parameters against the radial moments of the rare-earth ions, and secondly by plotting the best-fit crystal field parameters against the cell volumes obtained from Ref. [7]. The fact that these parameters fall fairly well on a line indicates that the CEF parameters vary in a systematic way as in the lanthanide contraction. The sign of the second-order CEF parameter correlates with the easy axis of the R 1:2:4 crystals. Plotted in Figs. 8–13 is a linear fit to these parameters. The quality of all the fits is fairly good except for the B_{46} parameter. Adjustment of this parameter to fall in line with the other B_{46} parameters resulted in a poor fit to the susceptibility data. The values of these fits are listed in Tables VIII and IX. The scaling relation developed in this work should allow one to scale across a

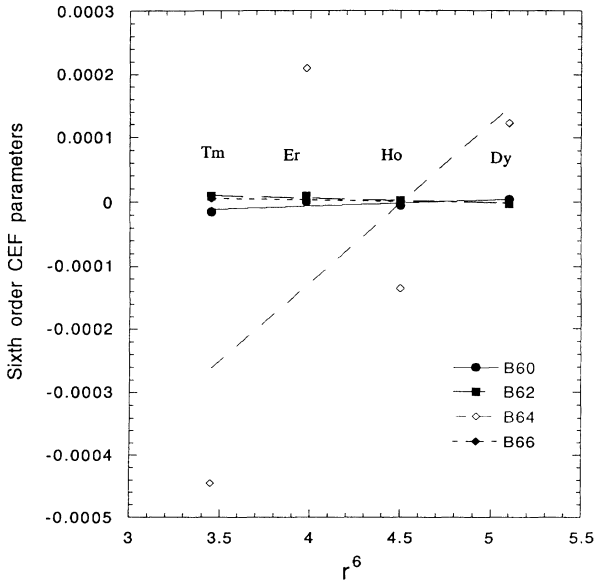

FIG. 10. Graph of sixth-order best-fit CEF parameters in meV vs sixth-order radial moment in units of a_0^{-2}.

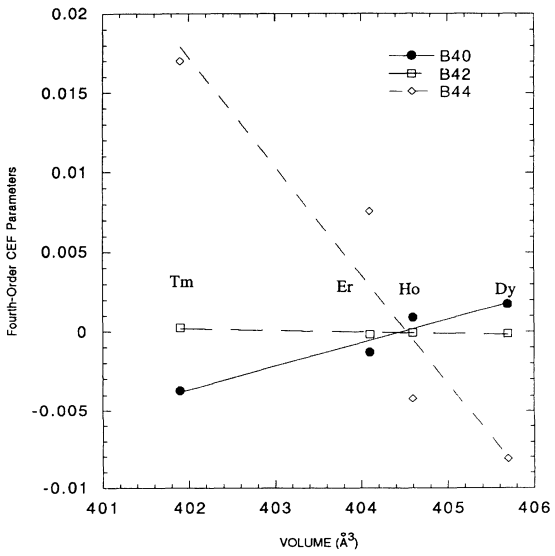

FIG. 12. Graph of fourth-order best-fit CEF parameters in meV vs cell volume in units of Å^3.

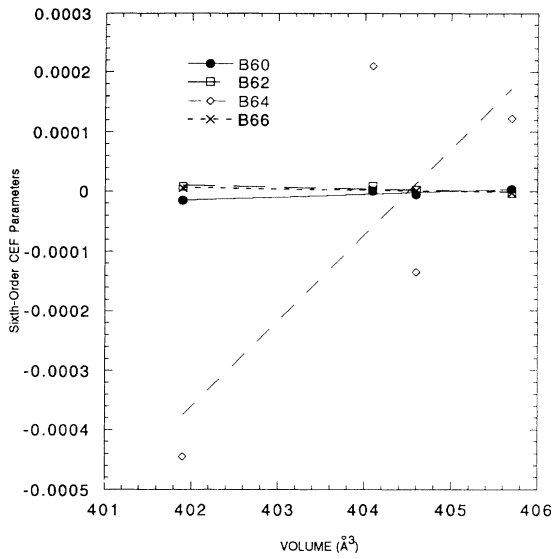

FIG. 13. Graph of sixth-order best-fit CEF parameters in meV vs cell volume in units of $Å^3$.

large part of the rare-earth series. The use of this scaling relation will allow one to generate a Hamiltonian from which other quantities of interest can be calculated, for instance, specific heat, scattering probabilities used in inelastic neutron scattering, as well as magnetization.

CONCLUSION

In order to determine the crystalline electric field and hence the energy-level splitting of a rare-earth ion in a 1:2:4 structure we have measured the magnetic susceptibility in the normal state along the three principal axes of single-crystal $RBa_2Cu_4O_8$ (where R=Y, Tb, Yb, Er, Gd, Dy, Ho, Dy, Tm). We then performed a theoretical fit using the Van Vleck formalism based on a crystal-field Hamiltonian developed from the Stevens equivalent operator method. Using as starting parameters results from published inelastic-neutron-scattering experiments, these crystalline-electric-field parameters were adjusted to minimize the χ^2 fit to the data. From our results a scaling relation has been developed for the crystal-field parameters across the rare-earth series in the 1:2:4 system. Its use should be of very broad scope.

ACKNOWLEDGMENTS

The authors would like to thank Lynn Soderholm for her help and discussion in the initial calculations performed in this work. This work was partially supported by the National Science Foundation through NSF cooperative agreement No. DMR-9016241. D.H.N. would like to thank the staff of the Material Science Division at Argonne National Laboratory for their hospitality during an extended visit.

[1]A. A. Abrikosov and L. P. Gorkov, Teor. Fiz. **39**, 1781 (1960) [Sov. Phys. JETP **12**, 1243 (1961)].
[2]R. M. Hazen *et al.*, Phys. Rev. B **35**, 7238 (1987).
[3]P. Marsh *et al.*, Nature **334**, 141 (1988).
[4]B. Dabrowski *et al.*, Physica C **193**, 64 (1992).
[5]U. Welp *et al.*, Physica C **161**, 1 (1989).
[6]U. Welp (unpublished).
[7]D. E. Morris *et al.*, Phys. Rev. B **39**, 7347 (1989).
[8]K. W. H. Stevens, Proc. Phys. Soc. London Sect. A **65**, 209 (1952).
[9]M. T. Hutchings, in *Solid State Physics: Advances in Research and Applications,* edited by H. Ehrenreich *et al.* (Academic, New York, 1964), Vol. 16, p. 227.
[10]L. Soderholm *et al.*, Phys. Rev. B **45**, 10 062 (1992).
[11]A. Furrer *et al.*, Phys. Rev. B **38**, 4616 (1988).
[12]G. H. Dieke, in *Spectra and Energy Levels of the Rare-earth Ions in Crystals,* edited by H. M. Crosswhite and H. Crosswhite (Interscience, New York, 1968).
[13]J. H. Van Vleck, *The Theory of Electric and Magnetic Susceptibilities* (Oxford University, London, 1932).
[14]W. H. Press, B. P. Flannery, S. A. Teukolsky, and W. T. Vetterling, *Numerical Recipes* (Cambridge University, Cambridge, 1986).
[15]K. N. R. Tayler and M. I. Darby, *Physics of Rare Earth Solids* (Chapman and Hall, London, 1972).
[16]R. Rosessli *et al.*, Phys. B **91**, 149 (1993).
[17]J. M. Ferreira *et al.*, Appl. Phys. A **47**, 105 (1988).
[18]P. Allenespach *et al.*, Phys. Rev. B **39**, 2226 (1989).